Supplement of Biogeosciences, 21, 4317–4339, 2024
https://doi.org/10.5194/bg-21-4317-2024-supplement

Supplement of

Tracing rate and extent of human-induced hypoxia during the last 200 years in the mesotrophic lake, Tiefer See (NE Germany)

Ido Sirota et al.

Correspondence to: Ido Sirota (idosir@gfz-potsdam.de)

Figure S1 – varve counting and core correlation

Varve counting and core correlation of all the cores used in this study. Each core is presented as an assemblage of thin sections images, covering the entire varved interval (Unit V). The orange dots mark that counted calcite layers, each dot represents one year. In addition, the marker layers that were determined on the TSK11-K1 master core, are marked on all of the cores with their ages. The year of the onset of varve preservation appears at the base of the varved unit in each core.

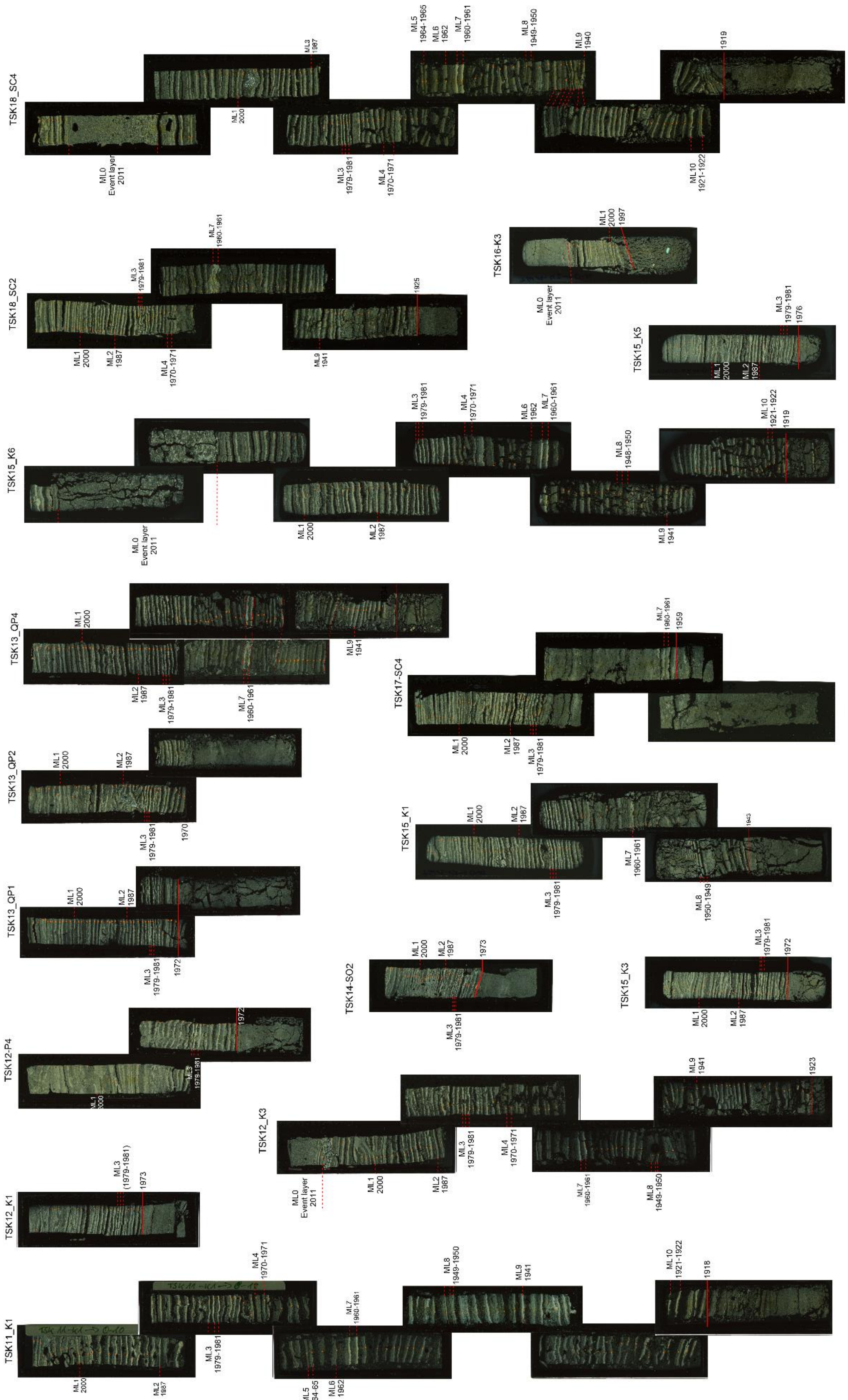

TSK18_SC4
ML0
Event layer
2011
ML1
2000
ML3
1987
ML3
1979-1981
ML4
1970-1971
ML5
1964-1965
ML6
1962
ML7
1960-1961
ML8
1949-1950
ML9
1940
1919
ML10
1921-1922
TSK18_SC2
ML1
2000
ML2
1987
ML3
1979-1981
ML4
1970-1971
ML7
1960-1961
ML9
1941
1925
TSK16-K3
ML0
Event layer
2011
ML1
2000
1997
TSK15_K5
ML1
2000
ML2
1987
ML3
1979-1981
1976
TSK15_K6
ML0
Event layer
2011
ML1
2000
ML2
1987
ML3
1979-1981
ML4
1970-1971
ML6
1962
ML7
1960-1961
ML8
1948-1950
ML9
1941
ML10
1921-1922
1919
TSK13_QP4
ML1
2000
ML2
1987
ML3
1979-1981
ML7
1960-1961
ML9
1941
TSK17-SC4
ML1
2000
ML2
1987
ML3
1979-1981
ML7
1960-1961
1959
TSK13_QP2
ML1
2000
ML2
1987
ML3
1979-1981
1970
TSK15_K1
ML1
2000
ML2
1987
ML3
1979-1981
ML7
1960-1961
ML8
1950-1949
1943
TSK13_QP1
ML1
2000
ML2
1987
ML3
1979-1981
1972
TSK14-SO2
ML1
2000
ML2
1987
ML3
1979-1981
1973
TSK15_K3
ML1
2000
ML2
1987
ML3
1979-1981
1972
TSK12-P4
ML1
2000
ML3
1979-1981
1972
TSK12_K3
ML0
Event layer
2011
ML1
2000
ML2
1987
ML3
1979-1981
ML4
1970-1971
ML7
1960-1961
ML8
1949-1950
ML9
1941
1923
TSK12_K1
ML3
(1979-1981)
1973
TSK11_K1
ML1
2000
ML2
1987
ML3
1979-1981
ML4
1970-1971
ML5
1964-65
ML6
1962
ML7
1960-1961
ML8
1949-1950
ML9
1941
ML10
1921-1922
1918

Figure S2. Crypto-tephra results and interpretation

The colorless glass shards from TSK12-K1_22-23cm and TSK13-QP1_19-20cm are similar in major element composition with both being rhyolitic (SiO_2: TSK12-K1_22-23cm 73.70 ± 0.60 wt.% 1 s.d.; TSK13-OP1_19-20cm 73.25 ± 0.95 wt.% 1 s.d.) and subalkaline with low K_2O (TSK12-K1_22-23cm 2.43 ± 0.05 wt.% 1 s.d.; TSK13-OP1_19-20cm 2.40 ± 0.02 wt.% 1 s.d.) and high CaO (TSK12-K1_22-23cm: 2.32 ± 0.22 wt.% 1 s.d.; TSK13-OP1_19-20cm: 2.56 ± 0.25 wt.% 1 s.d.; Fig. 2). Due to this distinct geochemistry and the chronostratigraphic position of these tephra peaks, we can confidently correlate these glass shards to the eruption of Askja AD 1875 (Fig. 1). This cryptotephra has already been found in Tiefer See in core TSK11-K3_33-34cm by Wulf et al. (2016) and is also found in many other sites throughout north-eastern Europe (e.g. Kinder et al., 2021). The figure shows a Bi-plots of selected major elements of glass shards from Tiefer See cores TSK-12 and TSK-13 with comparisons to Askja 1875 distal and proximal deposits (Bergman et al., 2004; Boygle, 2004; Davies et al., 2007; Kinder et al., 2021; Larsen et al., 1999; Pilcher et al., 2008; Stivrins et al., 2016; Wastegård, 2002, 2005; Watson et al., 2015; Wulf et al., 2016) and Hekla 1845 distal (Wastegård, 2002; Watson et al., 2015).

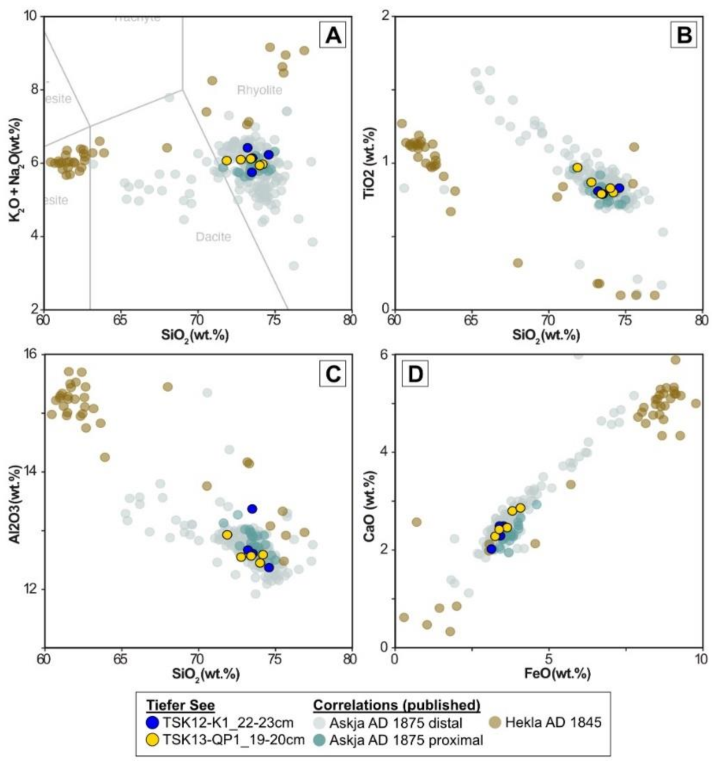

Figure S3. Lacustrine fill

The Holocene lacustrine sedimentary fill in the lake was deposited on top glacial sediments since the lake basin is formed within a subglacial channel system. Most of the pre-Holocene sediments are fluvioglacial sands but at two locations remains of glacial till that were not eroded by fluvial processes appear elevated and close to the present-day lake bottom. These areas are clearly visible in the sediment seismic image as black spots because of the higher density of the till compared to the sands and organic-rich Holocene lacustrine sediments. Core TSK16-K3 has been obtained from above the till remain in the northern part of the basin confirming till in 62 cm sediment depth. Thus, at this particular location glacial till has been recovered that has a very different geochemical composition as reflected by the XRF data.

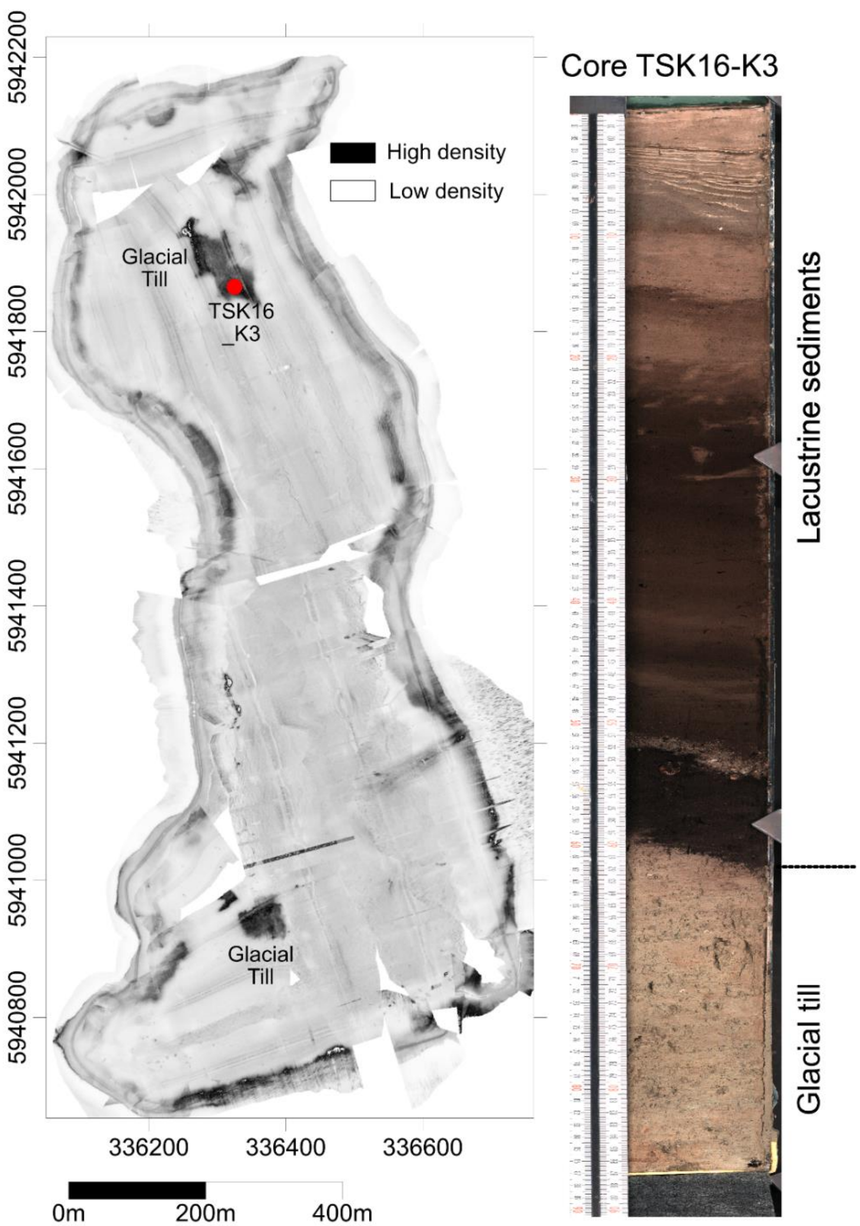

Figure S4. TOC in sediment trap data

Total organic carbon (TOC) flux, content and $\delta^{13}C_{org}$ of sediments from the hypolimnion of the lake are presented for the period of 2015-2021. Active sedimentation was monitored in order to identify the properties of the TOC in the lake. Sediment sampling is conducted at intervals of 15 days with an automated sequential trap (Technicap PPS 3/3; active area 0.125 m2) equipped with 12 sample bottles.
The sediments from the traps were freeze-dried and weighed to determine the dry deposition (i.e. sediment flux: g m–2 d–1). Afterwards, the samples were ground and homogenized. Prior to determination of TOC, 0.2 mg sample aliquots were in situ decalcified in Ag capsules (20% HCl and drying at 75 °C), also in replicates. TOC was measured on in-situ calcified samples using a Carlo Erba NC-2500 elemental analyzer. All process and analytical measurements were done at the laboratories of section 4.3 of the GFZ Potsdam center of geosciences, Potsdam, Germany.

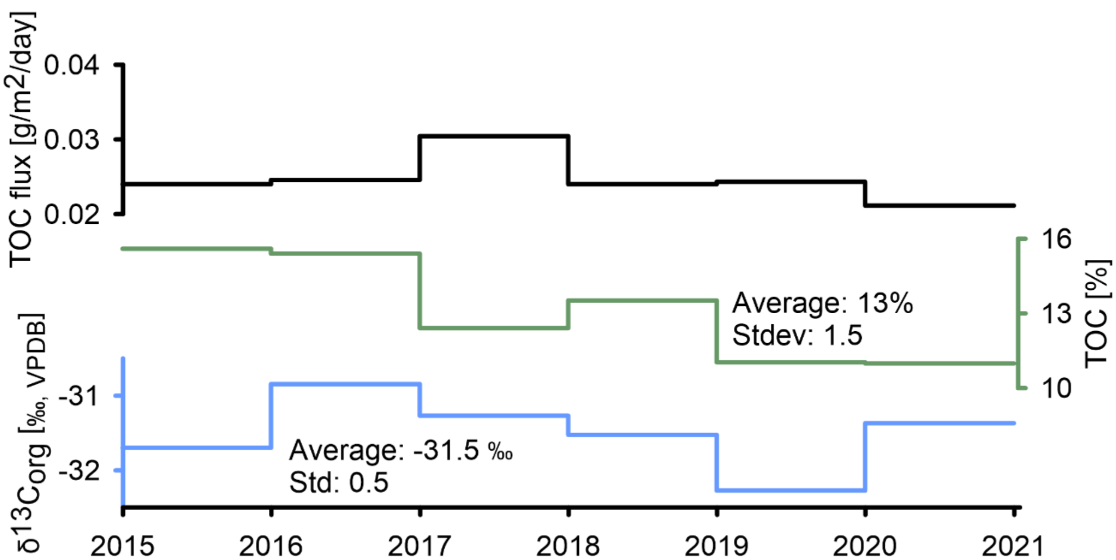

Table S1.

List of marker layers (ML) in cores TSK11-K1 and TSK18-SC4.

#Marker layer	Description	Number of varves from the previous ML	Age (year CE)
ML0	Mixed event layer	Observed in TSK18-SC4	2011
ML1	Clear calcite layer	10 (from the core top)	2000
ML2	Clear calcite layer	12	1987
ML3	Three distinct calcite layers	5	1979-81
ML4	Two brown (OM) layers in between thick diatom layer	7	1970-71
ML5	A brown (OM) layer in between thick diatom layers	4	1964-65
ML6	A clear calcite layer with a brown layer (OM) on top	1	1962
ML7	Two of thick calcite layers	0	1960-61
ML8	Three brown layers (OM)	9	1949-50
ML9	A thick calcite layer with a brown layer in the varve below	7	1941
ML10	Two thick calcite layers	18	1921-22
Varves base		3	1918

Table S2.

Non-normalized major elements for the peaks analyzed in this study. Values referred to in text are normalized to 100% and with the removal of volatiles.

Site	Core	Al_2O_3	K_2O	FeO	Na_2O	CaO	SiO_2	MgO	TiO_2	MnO	P_2O_5	Cl	Analytical total
TSK12-K1	22-23cm	12.50	2.44	3.49	3.65	2.47	72.90	0.68	0.78	0.10	0.12	0.03	99.16
TSK12-K1	22-23cm	12.59	2.42	3.37	3.96	2.47	72.74	0.75	0.80	0.09	0.12	0.04	99.36
TSK12-K1	22-23cm	13.21	2.33	3.38	3.35	2.26	72.61	0.61	0.78	0.10	0.13	0.04	98.80
TSK12-K1	22-23cm	12.08	2.40	3.06	3.68	1.97	72.82	0.60	0.81	0.10	0.09	0.04	97.64
TSK13-OP1	19-20cm	12.49	2.40	3.22	3.52	2.26	73.59	0.65	0.80	0.09	0.14	0.04	99.19
TSK13-OP1	19-20cm	12.51	2.40	3.80	3.68	2.79	72.52	0.82	0.87	0.08	0.15	0.03	99.65
TSK13-OP1	19-20cm	12.58	2.38	3.64	3.75	2.46	73.50	0.72	0.79	0.10	0.15	0.04	100.11
TSK13-OP1	19-20cm	12.36	2.37	3.35	3.53	2.40	73.44	0.68	0.82	0.10	0.14	0.05	99.24
TSK13-OP1	19-20cm	12.76	2.38	4.02	3.61	2.82	70.93	0.85	0.96	0.12	0.20	0.07	98.71

Table S3.

Secondary standards ran alongside the unknown samples of Tiefer See to ensure precision and accuracy of results

Standard	Al_2O_3	K_2O	FeO	Na_2O	CaO	SiO_2	MgO	TiO_2	MnO	P_2O_5	Cl	Analytical total
Lipari	13.05	5.08	1.45	4.03	0.75	73.29	0.04	0.14	0.06	0.03	0.32	98.24
Gor-132-G	10.88	0.03	10.21	0.82	8.47	45.47	22.46	0.31	0.15	0.05	0.00	98.86
St-Hs-6-80-G	17.78	1.30	4.40	4.41	5.25	63.72	2.05	0.72	0.08	0.17	0.04	99.92
ATHO-G	12.28	2.67	3.28	3.67	1.76	75.50	0.12	0.25	0.08	0.03	0.05	99.69

Table S4.

Chironomids counts in cores TSK15-K5 and TSK18-SC4 with division into identified chironomids species. See separate file.

References

Bergman, J., Wastegård, S., Hammarlund, D., Wohlfarth, B., and Roberts, S. J.: Holocene tephra horizons at Klocka Bog, west-central Sweden: aspects of reproducibility in subarctic peat deposits, J Quat Sci, 19, 241–249, https://doi.org/10.1002/jqs.833, 2004.

Boygle, J.: Towards a Holocene tephrochronology for Sweden: geochemistry and correlation with the North Atlantic tephra stratigraphy, J Quat Sci, 19, 103–109, https://doi.org/10.1002/jqs.811, 2004.

Davies, S. M., Elmquist, M., Bergman, J., Wohlfarth, B., and Hammarlund, D.: Cryptotephra sedimentation processes within two lacustrine sequences from west central Sweden, Holocene, 17, 319–330, https://doi.org/10.1177/0959683607076443, 2007.

Kinder, M., Wulf, S., and Appelt, O.: Detection of the historical Askja 1875 and modern Icelandic cryptotephras in varved lake sediments – results from a first systematic search in northern Poland, J Quat Sci, 36, 1–7, https://doi.org/10.1002/jqs.3259, 2021.

Larsen, G., Dugmore, A., and Newton, A.: Geochemistry of historical-age silicic tephras in Iceland, Holocene, 9, 463–471, https://doi.org/10.1191/095968399669624108, 1999.

Pilcher, J., Bradley, R. S., Francus, P., and Anderson, L.: A Holocene tephra record from the Lofoten Islands, Arctic Norway, Boreas, 34, 136–156, https://doi.org/10.1111/j.1502-3885.2005.tb01011.x, 2008.

Stivrins, N., Wulf, S., Wastegård, S., Lind, E. M., Alliksaar, T., Gałka, M., Andersen, T. J., Heinsalu, A., Seppä, H., and Veski, S.: Detection of the Askja AD 1875 cryptotephra in Latvia, Eastern Europe, J Quat Sci, 31, 437–441, https://doi.org/10.1002/jqs.2868, 2016.

Wastegård, S.: Early to middle Holocene silicic tephra horizons from the Katla volcanic system, Iceland: New results from the Faroe Islands, J Quat Sci, 17, 723–730, https://doi.org/10.1002/jqs.724, 2002.

Wastegård, S.: Late Quaternary tephrochronology of Sweden: a review, Quaternary International, 130, 49–62, https://doi.org/10.1016/j.quaint.2004.04.030, 2005.

Watson, E. J., Swindles, G. T., Lawson, I. T., and Savov, I. P.: Spatial variability of tephra and carbon accumulation in a Holocene peatland, Quat Sci Rev, 124, 248–264, https://doi.org/10.1016/j.quascirev.2015.07.025, 2015.

Wulf, S., Dräger, N., Ott, F., Serb, J., Appelt, O., Guðmundsdóttir, E., van den Bogaard, C., Słowiński, M., Błaszkiewicz, M., and Brauer, A.: Holocene tephrostratigraphy of varved sediment records from Lakes Tiefer See (NE Germany) and Czechowskie (N Poland), Quat Sci Rev, 132, 1–14, https://doi.org/10.1016/j.quascirev.2015.11.007, 2016.